FLUIDIZED BED CONVERSION CONFERENCE 2022
8-11th May 2022, Chalmers University of Technology (Sweden)

Binary mixtures of biomass and inert components in fluidized beds: experimental and neural network exploration

Paola Brachi[1], Riccardo Chirone[1], Roberto Chirone[2], Antonio Coppola[1], Vincenzo Del Duca[1], Michele Miccio[3], Giovanna Ruoppolo[1]

[1] *Istituto di Scienze e Tecnologie per l'Energia e la Mobilità Sostenibili – Consiglio Nazionale delle Ricerche, Piazzale V. Tecchio 80, 80125 Napoli, Italy*

[2] *Dipartimento di Ingegneria Chimica, dei Materiali e della Produzione Industriale (DICMaPI) Università degli Studi di Napoli Federico II, Piazzale V. Tecchio 80, 80125 Napoli, Italy*

[3] *Dipartimento di Ingegneria Industriale (DIIn), Università degli Studi di Salerno, via Giovanni Paolo II 132, 84084 Fisciano (SA), Italy*

Corresponding Author: Michele Miccio, mmiccio@unisa.it

Abstract

Considering the little understanding of the hydrodynamics of multicomponent particle beds involving biomass, a detailed investigation has been performed, which combines well-known experimental and theoretical approaches, relying, respectively, on conventional pressure drop methods and artificial neural network (ANN) techniques. Specific research tasks related to this research work include: i. to experimentally investigate by means of visual observation the mixing and segregation behavior of selected binary mixtures when varying the biomass size and shape as well as the properties (size and density) of the granular solids in cold flow experiments; ii. to carry out a systematic experimental investigation on the effect of the biomass weight and volume fractions on the characteristic velocities (e.g., complete fluidization velocity and minimum slugging velocity) of the investigated binary mixtures in order to select the critical weight fraction of biomass in the mixtures beyond which the fluidization properties deteriorate (e.g., channeling, segregation, slugging); iii. to analyze the results obtained in about 80 cold flow experiments by means of ANN techniques to scrutinize the key factors that influence the behavior and the characteristic properties of binary mixtures. Experimental results suggest that the bed components' density difference prevails over the size difference in determining the mixing/segregation behavior of binary fluidized bed, whereas the velocities of minimum and complete fluidization increase with a growing biomass weight fraction in the bed. The training of ANNs demonstrated good performances for both outputs (U_{mf} and U_{cf}); in particular, the best predictions have been obtained for U_{mf} with a MAPE[1]<4% (R^2=0.98), while for U_{cf} the best ANN returned a MAPE of about 7% (R^2=0.93). The analysis on the importance of each individual input on ANN predictions confirmed the importance of particle density of the bed components. Unexpectedly, results showed that morphological features of biomass have a limited importance on U_{cf}.

Keywords: Fluidization**,** Binary mixtures, Artificial neural network, Segregation, Mixing, Canonical Correlation Analysis.

1. Introduction

Several unique operational advantages, like fuel flexibility, uniform temperatures, intense solids mixing and efficient heat transfer, have made the fluidized beds the most efficient and widely applied reactors for the conversion of biomass into useful forms of bioenergy and/or biofuels. In spite of this, relatively few authors have so far deepened the study of the relevant flow characteristics of fluidized beds involving biomass particles [1], which are critical for the success of novel energy-related processes as

[1] MAPE: mean average percentage error

well as improvement of the performance of the existing ones. So far, most fundamental work on binary bed fluidization is, in fact, mostly focused on dry and dense spherical particles of narrow size distributions, with limited extension to other regular shapes [1], which do not at all reflect the characteristics of the biomass particles. Further research is therefore needed to provide a general understanding of interactions among heterogeneous particles, as well as practical tools to predict the hydrodynamics behavior of binary mixture involving biomass. The development of models based on physicochemical relations are, however, expensive in terms of time and money. In this framework, artificial intelligence, and in particular machine learning (ML) techniques, has the potential to overcome the limitations of first principles models, as it can learn complex behaviors from dataset with a low-cost development of the model. Among several ML techniques, artificial neural networks (ANNs) are extensively used in different fields such as machine diagnostics, pattern recognition, quality control as well as fitting experimental data, gaining in the years a relevant role also in chemical engineering [2].
Also in the field of multiphase systems, the scientific community implemented different ML techniques to solve problems related to the prediction of specific parameters and how the material properties, the operating conditions and the equipment features influence these latter [3–12]. In this regards, Chew & Cocco [3,4] tried to use ML techniques (random forest (RF) and ANN) to understand and predict the hitherto not fully understood fluidization phenomena in circulating fluidized bed (CFB) systems. They used RF to investigate the relative influence of the process variables (material type and operating conditions) on the local mass flux, concentration, segregation and cluster characteristics. The results revealed how some variables are mainly influenced by geometric characteristics of the CFB systems, others strongly depend on operating conditions while still others, which are more or less equally influenced by all process variables. Conversely, the ANN was trained to predict the output variables giving back good prediction for some output with a mean NRMSE[2] value of about 0.04 and R^2 values above 0.9; for other output variables the ANN gave poor prediction, probably due to the lack of accounting of some reactor characteristics. Despite this missing information, the authors improved the poor prediction trainings with a more accurate choice/elimination of the input variables based on the ranking of importance by the RF method. ANN was also used by Fu et al. [5] to predict the macroscopic flow characteristics of particles in a bubbling fluidized bed, as function of particle properties, gas velocity, gas distributor, axial position and radial position. The ANN training shows that the flow characteristics are affected by several of factors with the following importance rank Axial position > Radial position > Gas properties > Gas distributor. Moreover, the results obtained from ANN were compared with theoretical calculations based on constitutive equations, which have been less accurate than ML technique. Instead, Perrazzini et al. [12] tested the ability of ANN to estimate drying kinetics in fixed, fluidized and vibro-fluidized bed dryers under different operating conditions. The results show that the model is able to estimate new patterns just for the cases in which the database refers to a single type of dryer. Conversely, the developed networks showed difficulty to learn multiple patterns from different type of dryers, resulting in predictions with low accuracy, because information in the dataset about the different gas-solid contact were not present. This demonstrates the importance to choose proper input variables in the dataset for an efficient prediction. As concern the prediction of the minimum fluidization velocity (U_{mf}), several authors used different ML techniques with a preponderance of ANNs. Targino and coworkers [9] trained ANN to evaluate the key factors that influence the condition of minimum fluidization of acai berry residues. The performances of trained ANN have been encouraging, because able to predict in a quite fairly good way the minimum fluidization velocity for conditions not present in the original dataset, demonstrating the potentialities of the ANN. It is worth to cite the work of Zhou and colleagues [10], because they combine the application of ANNs for U_{mf} with a text mining approach for the automatic creation of the dataset. The text mining analyzed about 40,000 papers and the result was a dataset formed by more than 1400 observations, which include particle and fluid characteristics and operating conditions. The predictions of the ANN offer a better capability to estimate U_{mf} with respect to Ergun and Wen−Yu correlation. Other authors focused their attention on the evaluation of the U_{mf} in spouting beds [7,8] concluding that the ANNs provide reliable predictions, better than empirical correlations. Rushd et al. [6] compared different ML techniques used singularly or in combinations for the estimation of the terminal settling velocity of spherical and non-spherical particles in Newtonian and non-Newtonian fluid. In particular, the results highlighted that the RF regression model provided the best performance compared the other models used singularly, while the combination of different ML techniques performed very similar to the RF model but showed a more elevated computational complexity.
In an attempt to tackle this knowledge gap, an experimental investigation aiming at analyzing the fluidization behavior of highly poly-disperse binary mixtures consisting of small and dense inert particles

[2] normalized root mean-squared error

mixed with less dense and coarse pieces of biomass fuels has been performed by using a borosilicate glass fluidization column (0.10 m ID) equipped with a 4-mm-thick sintered-glass gas distributor and the results are presented in this paper. Specifically, peels of fresh oranges, which mimic the solid by-products of orange fruit processing, and tomato peels, which are the by-product of the peeling of tomatoes used for canning, were used as the biomass component due to the increasingly interest they are gaining as a potential feedstock for bioenergy and biofuels productions [13,14].
Four

continuously recorded and the onset of both the conditions of minimum (U_{mf}) and complete fluidization (U_{cf}) were comparatively determined by means of the conventional graphical methods, whereas the visual observation was used to identify the onset of the undesired slugging regime and segregation phenomena. For each of the investigated binary mixtures (e.g., UFA/FOP, FA/FOP, FS/FTP and CS/FTP) several fluidization tests were performed by increasing the biomass weight fraction (X_B) into the bed; this approach made possible to both study the effect of the bed content on the characteristic velocities of the binary systems under study (i.e., minimum and complete fluidization velocities) and determine the critical value of X_B beyond which the fluidization pattern deteriorates (e.g., channeling, segregation, slugging). As for fluidization tests relating to binary mixtures, the initial arrangement of the bed was that with teh bed components completely segregated and the biomass particles on the top (see Figure 1B). Starting from this fixed bed configuration, first the airflow rate was quickly set at 1500 Nl/h (corresponding to a superficial gas velocity of about 5 cm/s) and then gradually increased until a slugging or turbulent regime was observed. In most of the performed experimental runs, an air flow rate in the order of 1500 Nl/h proved to be sufficient to ensure a gradual transition (in less than 2 minute) from the initial fully segregated fixed bed configuration (Figure 1B) to a well-mixed regime (Figure 1C) characterized by a uniform distribution of particles in the bed, as showed by the snapshots in Figure 1, which refers to CA/FOP-22 binary mixture. However, in general, both the critical air flow rate and time required to reach a well-mixed regime slightly increased by increasing the biomass weight fraction in the bed for each of the investigated binary mixtures [16]. It is worth noting that if a too high initial air flow rate was adopted, the system exhibited an almost plug-flow behavior, which means that all particles were transported out of the bed with little back-mixing. The values of the U_{mf} and the U_c were measured upon decreasing the fluidization gas flow rate to avoid dependence on the initial bed configuration. Hence, during each experiment, starting from the above-mentioned well-mixed regime, the air flow rate was gradually decreased to zero and the pressure drop across the bed continuously recorded.

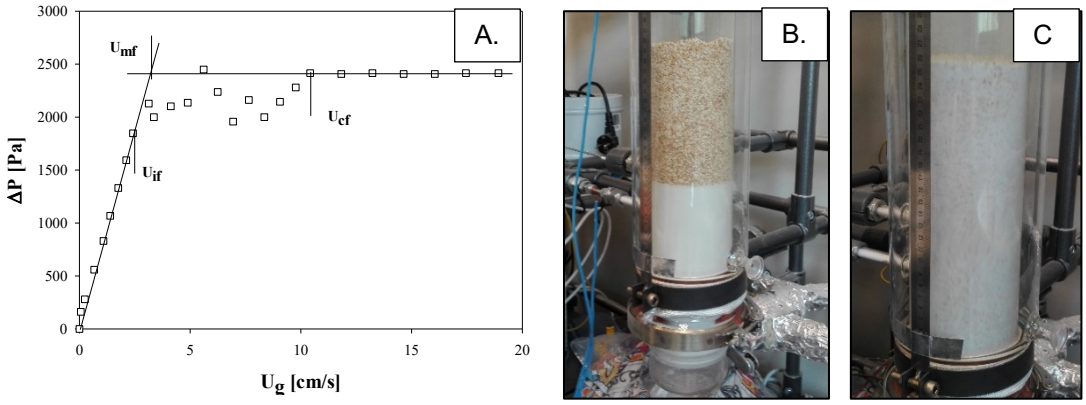

Figure 1. A.) Pressure drop diagram of a two component mixture obtained by the complete mixing of spheres differing only in diameter (adapted from [20]**); B.) snapshot of the initial arrangement of the bed during the cold flow fluidization test performed on the CA/FOP-22 binary mixture: C.) snapshot of the CA/FOP-22 binary mixture "frozen" in a perfectly mixed condition by instantly bringing the fluidization gas flow to zero.**

2.4. Canonical Correlation Analysis and Artificial Neural Networks

In a first phase, the parameters used as inputs were: inert material density $\rho_{particle}$ (kg/m^3), inert Sauter diameter d_{Sauter}, biomass volume fraction in the bed (%vol.), biomass characteristic size (i.e., prevailing length L_b, mm), biomass particle density $\rho_{particle}$ (kg/m^3), biomass sphericity factor Φ_b. In a subsequent phase, CCA inputs were linearly combined and incremented with the following ones: inert material bulk density ρ_{bulk} (kg/m^3), biomass bulk density ρ_{bulk} (kg/m^3), biomass weight fraction in the bed (%wt.). On the other side, the outputs parameters were the minimum fluidization velocity U_{mf} and the complete fluidization velocity U_{cf}. About the calculation of Φ_b, fine orange peels present a pseudo-spheroidal shape with relative proportions of 1:1:2 [23], so a value of 0.93 was set; for coarse orange peels and fine tomato peels the shapes resembled rectangular parallelepipeds with relative proportions of 1:4:4 and 1:2:4, so the values of Φ_b were set 0.64 and 0.68, respectively. L_b was defined as the average maximum dimension of the biomass particle; so, for fine orange peels, coarse orange peels and fine tomato peels L_b was 1.41, 5.00 and 1.04 mm, respectively. The performance indicators are *MAE*, *MSE,*

SAE, MAPE and R^2 [3] calculated in the evaluation of the fluidization velocity but for simplification, only *MAPE* and R^2 have been reported here.

Canonical Correlation Analysis (CCA) is widely used to extract the correlated patterns between two sets of variables. CCA looks at two sets of variables for modes of maximum correlation between the two sets. Thus, CCA sits at the top of a hierarchy of regression models where it is able to manage multiple predictors (inputs) and multiple predictands (outputs). If x is the set of predictors and y the predictands, then CCA can be used to predict y when new observations of x become available [24]. In this study, CCA is used as a starting and comparative statistical advanced analysis to the ANNs, in terms of performance (*MAPE,* R^2), relative to the minimum and complete fluidization velocity, U_{mf} and U_{cf}. In this study, ANNs were used to predict the minimum fluidization velocity U_{mf} and the complete fluidization velocity U_{cf}. Input and output parameters used are the same used for CCA analysis. Specifically, an algorithm, called "netoptim", was conceived within the present research and implemented in Matlab to develop a large number of ANNs, with the goal of evaluating different choices such as: i.) the network type (*fitnet*, *feedforwardnet* and *cascadeforwardnet*); ii.) the number of neurons in the hidden layer (set, initially, equal to the number of inputs ± 3); iii.) the training function[4].

In this work, the authors decided to set up the transfer function as the hyperbolic tangent sigmoid, to avoid a further parameter to investigate.

3. Results and discussion

3.1. Experimental results - Dataset

Table 2 lists the values of the velocities of minimum and complete fluidization obtained for the investigated binary mixtures as borrowed from a previous study of the Authors [16].

Table 2. Experimental operating variables and binary mixture characteristic velocities

Binary mixtures	% wt. Biomass	%vol. Biomass	U_{mf}, cm/s	U_{cf}, cm/s	Binary mixtures	% wt. Biomass	%vol. Biomass	U_{mf}, cm/s	U_{cf}, cm/s
FS/COP-0	0	0.00	1.99	2.85	UFA/FOP-18	18.03	31.50	0.32	4.92
FS/COP-1	1.03	5.65	2.27	5.08	FA/FOP-0	0	0.00	0.68	2.04
FS/COP-2	2.04	10.69	2.35	5.62	FA/FOP-2	2.17	4.51	0.8	5.33
FS/COP-3	2.97	14.97	2.62	6.19	FA/FOP-4	4.1	8.34	0.73	5.33
FS/COP-4	4.18	20.05	3.17	6.63	FA/FOP-6	6.03	12.02	0.74	4.92
CS/COP-0	0	0.00	3.75	6.43	FA/FOP-8	8.03	15.67	0.74	4.92
CS/COP-1	1.04	5.57	4	5.24	FA/FOP-10	10.06	19.23	0.73	4.79
CS/COP-3	2.96	14.62	3.79	5.10	FA/FOP12	12.34	23.06	0.6	4.92
CS/COP-5	4.85	22.24	4.23	5.66	FA/FOP-14	14.16	25.99	0.66	4.92
FA/COP-0	0	0.00	0.68	2.04	FA/FOP-16	16.3	29.31	0.61	4.91
FA/COP-1	0.99	2.92	0.79	1.21	FA/FOP-18	18.18	32.11	0.55	5.31
FA/COP-3	2.91	8.27	0.76	1.72	FA/FOP-20	20.56	35.53	0.59	5.43
FA/COP-5	4.82	13.22	0.79	1.71	FA/FOP-22	22.07	37.61	0.57	5.68
FA/COP-7	6.61	17.56	0.77	2.04	FA/FOP-24	24.07	40.29	0.59	5.81
FA/COP-9	9.17	23.30	0.78	2.69	FA/FOP-26	26.27	43.13	0.6	6.60
FA/COP-11	10.77	26.64	0.76	2.99	FA/FOP-28	28.25	45.60	0.81	6.96
FA/COP-12	12.31	29.70	0.77	3.00	CA/FOP-0	0	0.00	3.05	5.94
FA/COP-14	13.86	32.62	0.84	3.01	CA/FOP-2	2.17	4.75	3.21	5.19
FA/COP-15	15.31	35.23	0.93	3.31	CA/FOP-4	4.06	8.69	3.21	4.92
FA/COP-17	16.73	37.68	0.86	3.94	CA/FOP-6	6.01	12.57	3.24	5.18
FA/COP-18	18.1	39.94	0.95	4.23	CA/FOP-8	8.05	16.44	3.55	5.94
CA/COP-0	0	0.00	2.96	5.94	CA/FOP12	11.5	22.61	4.15	4.92
CA/COP-2	2.01	6.12	3.07	4.53	CA/FOP-14	14.29	27.26	5.63	5.19
CA/COP-4	4.09	11.93	3.09	4.53	CA/FOP-18	18.8	34.23	5.23	6.17
CA/COP-6	6.08	17.06	3.1	4.82	CA/FOP-22	22.36	39.30	6.37	6.52
CA/OP-8	8.05	21.76	3.24	5.53	CA/FOP-24	24.05	41.58	7.38	7.70

[3] MAE=mean absolute error; MSE=mean square error; SAE= sum absolute error; MAPE=mean absolute percentage error; R^2=coefficient of determination.

[4] Levenberg-Marquardt, Bayesian regularization backpropagation, BFGS quasi-Newton backpropagation, Resilient backpropagation, Scaled conjugate gradient backpropagation, Conjugate gradient backpropagation with Powell-Beale restarts, Conjugate gradient backpropagation with Fletcher-Reeves updates, Conjugate gradient backpropagation with Polak-Ribiére updates, One-step secant backpropagation, Gradient descent with momentum and adaptive learning rate backpropagation, Gradient descent with momentum backpropagation, Gradient descent backpropagation;

Binary mixtures	% wt. Biomass	%vol. Biomass	U_{mf}, cm/s	U_{cf}, cm/s	Binary mixtures	% wt. Biomass	%vol. Biomass	U_{mf}, cm/s	U_{cf}, cm/s
CA/COP-10	10.15	26.41	3.29	5.38	FSS/TP-0	0	0.00	1.99	2.85
CA/COP-12	12.24	30.70	3.38	5.58	FSS/TP-1	1	13.20	2.14	6.43
FA/COP-14	14.31	34.66	3.49	5.58	FSS/TP-2	2	23.50	3.65	6.45
CA/COP-16	16.36	38.33	3.42	6.10	FSS/TP-3	3.5	35.31	8.22	9.84
UFA/FOP-0	0	0.00	0.35	1.04	FSS/TP-5	5.2	45.22	8.48	10.69
UFA/FOP-2	2.17	4.43	0.34	4.12	FSS/TP-9	9	59.81	12.33	12.74
UFA/FOP-4	4.13	8.26	0.34	4.28	CSS/TP-0	0	0.00	3.75	6.43
UFA/FOP-6	6.06	11.88	0.35	3.84	CSS/TP-1	1	12.92	6.1	8.00
UFA/FOP-8	8.05	15.47	0.36	4.13	CSS/TP-2	2	23.06	8.3	9.50
UFA/FOP-10	10.16	19.12	0.38	4.27	CSS/TP-3	3.5	34.75	10.7	11.30
UFA/FOP-12	12.04	22.25	0.28	4.41	FA/TP-1	1	7.37	0.87	2.69
UFA/FOP-14	14.06	25.49	0.38	5.67	FA/TP-2	2	13.84	0.92	2.69
UFA/FOP-16	16.26	28.87	0.37	5.33	FA/TP-3	3	19.58	1.15	3.01

3.2. Modeling results

Table 3 reports the results of the CCA analysis carried out for U_{mf} and U_{cf}, in terms of MAPE for different attempts (tests 1-5) considering different combinations of input variables. Some inputs are fixed in all tests, such as the particle density of inert and biomass (ρ^I_{part} and ρ^B_{part}), the Sauter diameter of the inert (d^I_{Sauter}), the max average length (L_B) and the sphericity (Φ_B) of the biomass. Instead, the bulk density of inert and biomass (ρ^I_{bulk} and ρ^B_{bulk}) was considered only for tests 3 and 4, while the biomass fraction in the bed was reported in mass for tests 1 and 3, and in volume for tests 2 and 4, in order to evaluate which of the 2 variables has a positive effect on the performance of the statistical analysis. Finally, for the test 5 the effect of the biomass fraction in the bed was considered both by weight and by volume.

Table 3. MAPE of U_{mf} and U_{cf} obtained by CCA as a function of different set of inputs.

	Inert			Biomass				Biomass fract.		MAPE, %	
Test #	ρ^I_{bulk}	ρ^I_{part}	d^I_{Sauter}	ρ^B_{bulk}	ρ^B_{part}	L_B	Φ_B	$\%w$	$\%vol$	U_{mf}	U_{cf}
1	-	×	×	-	×	×	×	×	-	65.54	20.31
2	-	×	×	-	×	×	×	-	×	76.02	17.98
3	×	×	×	×	×	×	×	×	-	65.53	20.24
4	×	×	×	×	×	×	×	-	×	75.98	18.18
5	-	×	×	-	×	×	×	×	×	40.72	17.52

In general, the CCA shows poor performance for U_{mf}: a positive effect occurs when the biomass fraction (% wt.) in the bed is present among the inputs (tests 1 and 3), on the contrary the biomass fraction in the bed by volume tends to have a negative effect (test 2 and 4). However, a substantial improvement, even if the MAPE remains very high (>40%), occurs when both biomass fractions are used as inputs. The main difficulty of the CCA is found for low U_{mf} values (<1 cm/s), which mainly concerns mixtures where the inert is alumina below 150 μm. Probably this is related to the fact that such a solid belongs to the Geldart A particle classification, which determines a non-uniform fluidization condition.
Conversely, the performances on U_{cf} were much better, even if the effect of the biomass fraction is opposite with respect to that found for U_{mf}. Actually, the best results were obtained when the volume value was used (tests 2 and 4), obtaining MAPEs of approximately 18%; instead, the utilization of the weight fraction triggers an increase in the error of about 2 % points (tests 1 and 3). The presence of both fractions improves performance slightly (test 5). In conclusion, the best performance of CCA were MAPE values of 40.72% for U_{mf} and 17.52% for U_{cf}.
The set of inputs used for the training of the ANNs, the same for U_{mf} and U_{cf}, are those referred to the test 2 of the CCA. This choice was made because it gives the best combination between the number of inputs used and the value of the MAPE on U_{cf}, which is the variable of greatest interest here. Figure 2 shows the MAPE values resulting from the training of the three different networks with different architecture as a function of the number of neurons. The training function was also varied for each type of network and number of neurons, thus testing 12 different types, for a total of 216+216 neural networks trained for U_{mf} and U_{cf}. However, for the sake of clarity, only the best network obtained from the 12 different types of training functions is reported for each value of the number of neurons.

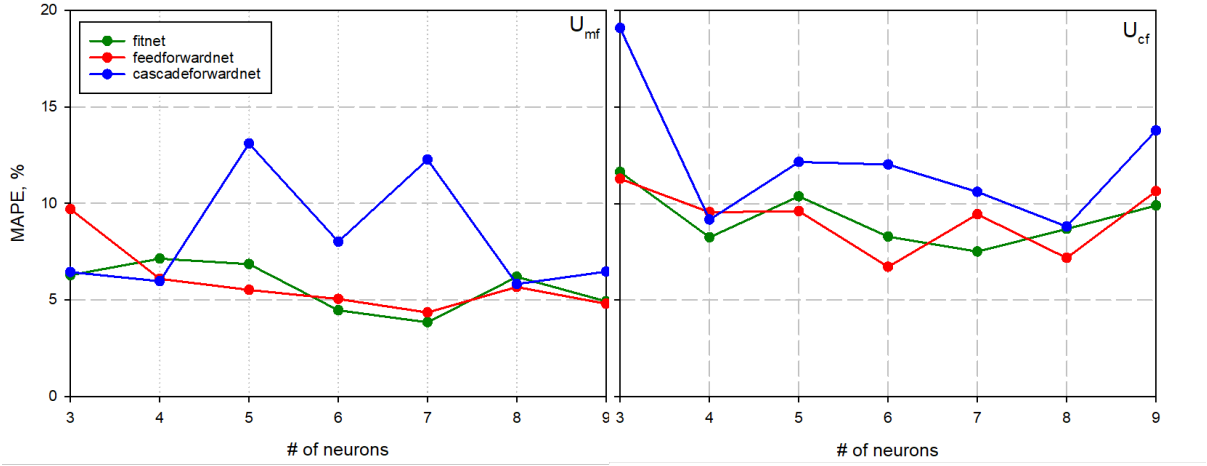

Figure 2. MAPE obtained by the training of the three different networks as a function of the number of neurons. U_{mf} on the left and U_{cf} on the right panel.

Unlike the CCA, the ANNs perform better on U_{mf} than on U_{cf}, even if in general it occurs that the ANNs have much better performances than the statistical analysis. For U_{mf} the best network was the fitnet with 7 neurons (training function based on Bayesian Regularization algorithm) with a MAPE value of about 4%.

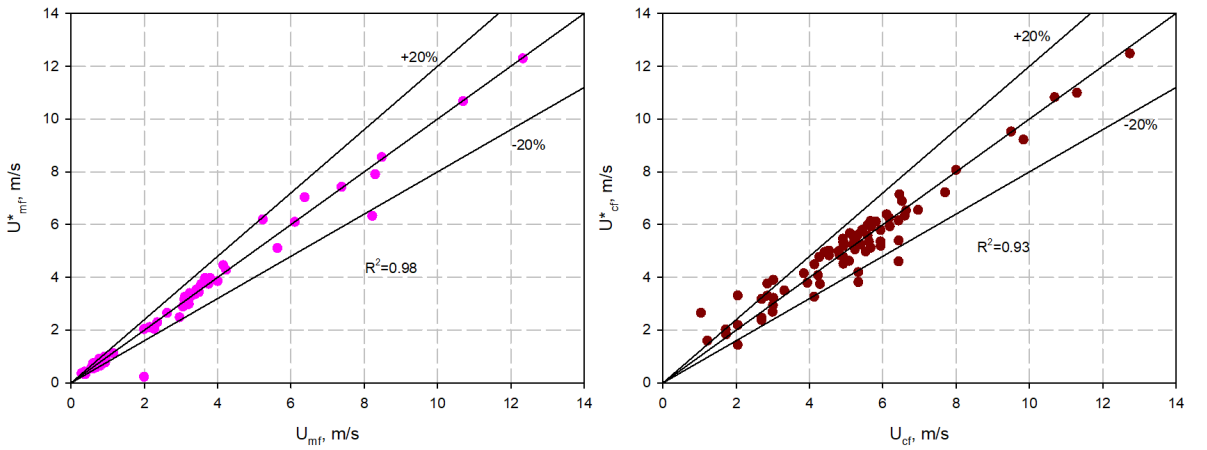

Figure 3. Comparison of the experimental results and predictions derived from the ANN. U_{mf} on the left and U_{cf} on the right panel.

Both the *fitnet* and the *feedforward* have a very similar trend unlike the *cascadeforwardnet*, which instead differs greatly from the other two, in particular, for intermediate values of the number of neurons (figure 2 on the left). The differences among the type on ANN becomes less evident for U_{cf} (figure 2 on the right). For U_{cf} the best ANN was the feedforward net with 6 neurons and, as in this case of U_{mf}, the best training function was the Bayesian Regularization algorithm. The MAPE obtained was about 6.71%. The best ANNs for the two outputs were further explored in detail in order to assess the impact of individual inputs on individual outputs. Figure 3 compares the real values of U_{mf} and U_{cf} with those expected (U^*_{mf} and U^*_{cf}) from the respective ANN networks. For U_{mf} it is possible to note that, also for low values, a satisfactory prediction is granted by the model, unlike the CCA, with a R^2 of 0.98. This demonstrates the great ability of ANN to manage complex relationships among physical properties. Also for U_{cf} the accordance with U^*_{cf} was very good, presenting a R^2=0.93. The application of the connection weight method [27–29] has permitted to evaluate the impact of individual inputs on the machine learning process (table 4). For U_{mf}, the particle density of the inert has the greatest impact of approximately 46%, followed by the sphericity (23.8%) and the characteristic size of the biomass (11.8%). The strong impact of the particle density of the inert is almost certainly because, when the minimum fluidization condition is reached, only the inert material begins to fluidize, while the biomass remains static in segregated conditions. U_{cf} is strongly dependent both on the particle density of the inert (31.4%) and on the volumetric fraction of the biomass in the bed (31.9%), as expected, and on the

particle density of the biomass itself (13.6%), albeit to a lesser extent. Vice versa, the characteristic size and sphericity of the biomass seem to play a marginal role; this result was certainly not predictable and would deserve further investigation.

Table 4. Relative importance of different inputs on U_{mf} and U_{cf}.

Variable	ρ^I_{part}	d^I_{Sauter}	ρ^B_{part}	L_B	Φ_B	$\%vol\ Biomass$
U_{mf}	46.8%	2.5%	3.8%	11.8%	23.8%	11.3%
U_{cf}	31.4%	9.4%	13.6%	6.9%	6.8%	31.9%

4. Conclusions

The present work investigated the fluidization and segregation behavior of poly-disperse binary mixtures of biomass and inert particles. In particular, air-dried orange and tomato peels were used as biomass feedstock whereas several granular solids with the same density but different size, or with the same size but different density were tested as inert bed component in order to determine the prevalence of the effect of either size or density on the fluidization and segregation behavior of the investigated binary systems. Tests at different weight fraction of the biomass in the bed were also performed for each of the investigated binary systems. Results suggest that the bed components' density difference prevails over the size difference in determining the mixing/segregation behavior of binary fluidized bed; on the other side, the velocities of minimum and complete fluidization increase when the biomass weight fraction in the bed is raised. The results from the experimental campaign have been used to create the dataset for the training of ANNs in MATLAB environment for predictions of U_{mf} and U_{cf} of binary mixtures. Before the development of ANNs, also a multivariate statistical analysis has been carried out by the implementation of Canonical Correlation Analysis (CCA). The results from CCA showed poor prediction performance particularly for U_{mf}, where fails have been particularly observed in the case of fine inert materials belonging to Geldart A group. Conversely, ANNs demonstrated good performances for both outputs, i.e., U_{mf} and U_{cf}; moreover, in opposite to CCA, best predictions have been obtained for U_{mf} with a MAPE<4% (R^2=0.98), whereas for U_{cf} the best ANN returned a MAPE of about 7% (R^2=0.93). The analysis on the relative importance of the different inputs showed interesting results, which deserve a deeper investigation. Indeed, U_{mf} depends strongly, as expected, on particle density of the inert solid and on the sphericity of the biomass, but the volumetric fraction (%) of the biomass in the bed and its characteristic length have had a lower impact on the results. This may be because, at minimum fluidization conditions, only the inert fluidizes, while the biomass remains static and segregated, and probably its presence in the bed represents, in a certain way, an obstacle to the movement of the inert solids. Conversely, the volumetric fraction of the biomass in the mixture becomes relevant for the prediction of U_{cf}, while the sphericity and the characteristic length of the biomass have a marginal role, as if the morphological characteristics of biomass become less important under conditions of complete fluidization of the bed.

References

[1] H. Cui, J.R. Grace, Fluidization of biomass particles: A review of experimental multiphase flow aspects, Chem. Eng. Sci. 62 (2007) 45–55. https://doi.org/10.1016/j.ces.2006.08.006.

[2] D.M. Himmelblau, Accounts of experiences in the application of artificial neural networks in chemical engineering, Ind. Eng. Chem. Res. 47 (2008) 5782–5796. https://doi.org/10.1021/ie800076s.

[3] J.W. Chew, R.A. Cocco, Application of machine learning methods to understand and predict circulating fluidized bed riser flow characteristics, Chem. Eng. Sci. 217 (2020) 115503. https://doi.org/10.1016/j.ces.2020.115503.

[4] J.W. Chew, R.A. Cocco, Do particle-related parameters influence circulating fluidized bed (CFB) riser flux and elutriation?, Chem. Eng. Sci. 227 (2020) 115935. https://doi.org/10.1016/j.ces.2020.115935.

[5] Y. Fu, S. Wang, X. Xu, Y. Zhao, L. Dong, Z. Chen, Particle flow characteristics in a gas-solid separation fluidized bed based on machine learning, Fuel. 314 (2022) 123039. https://doi.org/10.1016/j.fuel.2021.123039.

[6] S. Rushd, M.T. Parvez, M.A. Al-Faiad, M.M. Islam, Towards optimal machine learning model for terminal settling velocity, Powder Technol. 387 (2021) 95–107. https://doi.org/10.1016/j.powtec.2021.04.011.

[7] W. Zhong, X. Chen, J.R. Grace, N. Epstein, B. Jin, Intelligent prediction of minimum spouting velocity of spouted bed by back propagation neural network, Powder Technol. 247 (2013) 197–203. https://doi.org/10.1016/j.powtec.2013.07.022.

[8] J.F. Saldarriaga, F. Freire, J. Freire, Adjustment of the minimum spouting velocity in a conical

spouted bed from artificial neural networks, Chem. Eng. Trans. 70 (2018) 1243–1248. https://doi.org/10.3303/CET1870208.
[9] T.G. Targino, J.T. Freire, M.T.B. Perazzini, H. Perazzini, Fluidization design parameters of agroindustrial residues for biomass applications: experimental, theoretical, and neural networks approach, Biomass Convers. Biorefinery. (2021). https://doi.org/10.1007/s13399-021-01877-0.
[10] J. Zhou, D. Liu, M. Ye, Z. Liu, Data-Driven Prediction of Minimum Fluidization Velocity in Gas-Fluidized Beds Using Data Extracted by Text Mining, Ind. Eng. Chem. Res. 60 (2021) 13727–13739. https://doi.org/10.1021/acs.iecr.1c02307.
[11] B.A. Souto, V.L.C. Souza, M.T. Bitti Perazzini, H. Perazzini, Valorization of acai bio-residue as biomass for bioenergy: Determination of effective thermal conductivity by experimental approach, empirical correlations and artificial neural networks, J. Clean. Prod. 279 (2021). https://doi.org/10.1016/j.jclepro.2020.123484.
[12] H. Perazzini, M.T.B. Perazzini, L. Meili, F.B. Freire, J.T. Freire, Artificial neural networks to model kinetics and energy efficiency in fixed, fluidized and vibro-fluidized bed dryers towards process optimization, Chem. Eng. Process. - Process Intensif. 156 (2020) 108089. https://doi.org/10.1016/j.cep.2020.108089.
[13] P. Brachi, R. Chirone, F. Miccio, M. Miccio, G. Ruoppolo, Valorization of Orange Peel Residues via Fluidized Bed Torrefaction: Comparison between Different Bed Materials, Combust. Sci. Technol. 191 (2019) 1585–1599. https://doi.org/10.1080/00102202.2019.1582526.
[14] K. Midhun Prasad, S. Murugavelh, Experimental investigation and kinetics of tomato peel pyrolysis: Performance, combustion and emission characteristics of bio-oil blends in diesel engine, J. Clean. Prod. 254 (2020) 120115. https://doi.org/10.1016/j.jclepro.2020.120115.
[15] G. Bruni, R. Solimene, A. Marzocchella, P. Salatino, J.G. Yates, Self-segregation of high-volatile fuel particles during devolatilization in a fluidized bed reactor, 128 (2002) 11–21.
[16] P. Brachi, R. Chirone, F. Miccio, M. Miccio, G. Ruoppolo, Segregation and fluidization behavior of poly-disperse mixtures of biomass and inert particles, Chem. Eng. Trans. 57 (2017) 811–816. https://doi.org/10.3303/CET1757136.
[17] Y. Zhang, B. Jin, W. Zhong, Experimental investigation on mixing and segregation behavior of biomass particle in fluidized bed, Chem. Eng. Process. Process Intensif. 48 (2009) 745–754. https://doi.org/10.1016/j.cep.2008.09.004.
[18] K.L. Clarke, T. Pugsley, G.A. Hill, Fluidization of moist sawdust in binary particle systems in a gas-solid fluidized bed, Chem. Eng. Sci. 60 (2005) 6909–6918. https://doi.org/10.1016/j.ces.2005.06.004.
[19] B. Formisani, R. Girimonte, T. Longo, The fluidization process of binary mixtures of solids: Development of the approach based on the fluidization velocity interval, Powder Technol. 185 (2008) 97–108. https://doi.org/10.1016/j.powtec.2007.10.003.
[20] B. Formisani, R. Girimonte, Experimental analysis of the fluidization process of binary mixtures of solids, KONA Powder Part. J. 21 (2003) 66–75. https://doi.org/10.14356/kona.2003010.
[21] Y. Zhang, B. Jin, W. Zhong, Fluidization, mixing and segregation of a biomass-sand mixture in a fluidized bed, Int. J. Chem. React. Eng. 6 (2008). https://doi.org/10.2202/1542-6580.1809.
[22] A. Marzocchella, P. Salatino, V. Di Pastena, L. Lirer, Transient fluidization and segregation of binary mixtures of particles, AIChE J. 46 (2000) 2175–2182. https://doi.org/10.1002/aic.690461110.
[23] W.-C. Yang, Handbook of fluidization and fluid-particle systems, 2003. https://doi.org/10.1016/s1672-2515(07)60126-2.
[24] W.W. Hsieh, Nonlinear canonical correlation analysis by neural networks, Neural Networks. 13 (2000) 1095–1105. https://doi.org/10.1016/S0893-6080(00)00067-8.
[25] D. Serrano, D. Castelló, Tar prediction in bubbling fluidized bed gasification through artificial neural networks, Chem. Eng. J. 402 (2020). https://doi.org/10.1016/j.cej.2020.126229.
[26] J.H. Lee, J. Shin, M.J. Realff, Machine learning: Overview of the recent progresses and implications for the process systems engineering field, Comput. Chem. Eng. 114 (2018) 111–121. https://doi.org/10.1016/j.compchemeng.2017.10.008.
[27] J.D. Olden, D.A. Jackson, Illuminating the “black box”: Understanding variable contributions in artificial neural networks, Ecol. Modell. 154 (2002) 135–150.
[28] M. Gevrey, I. Dimopoulos, S. Lek, Review and comparison of methods to study the contribution of variables in artificial neural network models, Ecol. Modell. 160 (2003) 249–264. https://doi.org/10.1016/S0304-3800(02)00257-0.
[29] J.D. Olden, M.K. Joy, R.G. Death, An accurate comparison of methods for quantifying variable importance in artificial neural networks using simulated data, Ecol. Modell. 178 (2004) 389–397. https://doi.org/10.1016/j.ecolmodel.2004.03.013.